

# **Progress Report**

## **Development of a High Heat Flux Supercooler Using Carbon Foam**

**By**

**Walter Yuen**

**February, 12, 2008**

## **Introduction**

The objective of the work is to study the effectiveness of non-metallic foam as a heat spreader, liquid wick and heat sink material for electronic package with localized high heat flux (in the order of  $100 \text{ W/cm}^2$ ). Based on the geometry and heating requirement of a prototype package under consideration by an optoelectronic research group at UCSB, a “supercooler” is fabricated and its heat transfer performance is characterized experimentally. This report summarizes result of the current experimental and modeling efforts.

## **Design of the “supercooler”**

The specific optoelectronic package used as a basis of the design of the supercooler is shown in Figure 1. As shown in the figure, the dimension of the heating area is small (5.8 mm by 0.5 mm). The active material (InGaAsP and InP) is soldered to an AlN substrate which acts as a thermal spreader. The package is then soldered to kovar which is attached to a TE cooler for thermal control. The utilization of kovar (which has a small coefficient of thermal expansion) is generally considered to be necessary to maintain the necessary optical alignment of the different components of the package.

The “supercooler” designed specifically to meet the thermal requirement of the package is shown in Figure 2. The heating area is simulated by depositing a thin resistive layer (with a dimension of 0.5 mm by 5 mm) on an AlN substrate. In contrast to the actual package, the AlN substrate is brazed to a kovar slab only along its perimeter (approximately 1mm width). The interior of the substrate is brazed to a carbon foam tip. The carbon foam tip is a part of a carbon foam cylindrical shell which is soaked with liquid water to allow for both high heat transfer and thermal diffusion within the solid carbon matrix and two-phase boiling heat transfer in the porous region. The carbon foam shell is brazed to a copper cylindrical shell which provides the outside mechanical support and heat dissipating area for the supercooler.

An interior view of the supercooler and the relevant geometric dimensions are shown in Figure 3. The size of the copper cylinder is chosen so that there is sufficient area to dissipate the expected power input (1 to 10 W) by natural convection. The thickness of the carbon foam is selected largely based on practical constraints (the dimension of carbon foam available commercially and the brazing process). Prior to the experiment, the supercooler is sealed and evacuated down to  $10^{-6}$  Torr. A small amount of three-time de-ionized and de-gas water (20 gm) is then injected into the carbon foam shell to act as a two-phase coolant within the carbon foam.

## **Experiment**

The experimental set up is shown in Figure 4a. An high speed, high resolution infrared camera (SBF-180) is the primary temperature measurement equipment used in the experiment. The experimental setup, with the heating surface of the supercooler facing upward, together with the camera are shown in Figure 4b. Data were also obtained with the heating surface facing downward to assess the effect of gravity-driven buoyancy on the performance of the supercooler. Tests were conducted with applied

power of 4, 5 and 10 Watts to test the performance of the supercooler with increasing power dissipation.

## **Experimental Result**

### **Steady Heating**

The maximum temperature observed at the heating surface under a steady power input of 4 Watts and 10 Watts are shown in Figures 5a and 5b. At the initial stage of testing, there was a concern about securing good electrical contact to the thin resistive layer. A masking tape was wrapped around the mechanical contact on the side of the supercooler to ensure good electrical connection as shown in Figure 4a. This leads to additional thermal insulation and a slight increase in the maximum temperature as shown in Figure 5a. Subsequently, it was determined that good electrical contact was secured and all the remaining tests were conducted without the masking tape.

Data from the steady heating case show readily the high heat transfer capability of the supercooler. Based on the maximum temperature observed, the average heat transfer coefficient for the 4-W and 10-W case are approximately  $160 \text{ W}/(\text{m}^2\text{-K})$  and  $100 \text{ W}/(\text{m}^2\text{-K})$  respectively. The effect of the heater orientation is shown in Figure 5b for the 10-Watt case. In general, the effect of the heater orientation appears to be insignificant. The slight variation in the maximum temperature can probably attributed to experimental uncertainty (e.g. variation in setup, power input, ambient conditions, etc.).

Even for the steady heating case, the supercooler showed a remarkable cooling capability as the temperature of the surface drops rapidly (in about 1 sec.) after the power is turned off (see the 10 W case as shown in Figure 5b). This result demonstrates that the supercooler with carbon foam can lead to not only a high heat transfer coefficient during heating, it is also a thermal diffuser which can diffuse heat quickly away from the high temperature region when the heating is turned off.

### **Periodic Heating**

In view of the rapid temperature decrease observed in the steady heating tests, a series of tests were conducted to demonstrate the heat transfer behavior of the supercooler under the condition of a periodic heat input. Results for a maximum power input of 10 W and a regular square-wave heating input (i.e. the heater-on period equal to the heater-off period) are shown in Figure 6. It can be readily observed that the peak of the maximum temperature curve decreases with increasing frequency of the heating and the supercooler is effective in restoring the surface temperature close to the initial temperature ( $\Delta t < 10 \text{ C}$ ). The cooling rate for the three frequencies of periodic heating (0.5 Hz, 0.25 Hz and 0.17 Hz) shown in Figure 6 are  $17^\circ\text{C}/\text{sec}$ ,  $12^\circ\text{C}/\text{sec}$  and  $9^\circ\text{C}/\text{sec}$  respectively. Unfortunately, the current power supply used in the experiment can not generate periodic power input with a heating period less than 1 sec. The capability of the supercooler under power input with higher frequency will be considered in future work. Results for test conducted under different supercooler orientation are also shown in the same figure for comparison. The supercooler orientation has no impact on the heat transfer result.

Results of periodic heating tests with a constant heater-on period (3 sec.) and different heater-off period are shown in Figure 7. As expected, as the heater-off period decreases, the peak of the maximum temperature curve approaches to that of the steady state heating case. The supercooler, however, was still effective in significantly reducing the maximum temperature during the heater-off period.

Effect of the supercooler orientation for both the periodic heating and steady heating with a maximum power input of 10 W is illustrated by results shown in Figure 8. Periodic heating tests conducted with a maximum heat input of 5 W are shown in Figure 9. In general, these results demonstrate that the supercooler is effective in reducing the peak temperature during the heater-off period, independent of the supercooler orientation and the level of power input.

### **Analysis**

A thermal model of the supercooler is constructed using COMSOL to understand the controlling physics of the heat transfer processes. A schematic of the model is shown in Figure 10. For simplicity and to focus the modeling effort on the initial heating period, the current model simulates only the top part of the supercooler accounting for the carbon foam, kovar and AlN structural design. “Contact resistance” is included in the model to account for the the effect of joining (or brazing) different materials into one unit. The effect of the carbon foam and copper cylindrical shell will be important in the “long-time” thermal behavior of the supercooler. This effect will be considered in the future.

The current model also does not include the presence of liquid water in the carbon foam. The mechanism of two-phase flow and boiling in carbon foam is currently not well understood. Convective heat transfer within the foam is thus not included in this model. An effective heat transfer coefficient at the bottom surface of the carbon foam ( $h_b$ ) and an effective heat transfer coefficient at the top surface of the AlN surface ( $h_t$ ) are used to account for the overall heat dissipation from the supercooler. Due to this simplification, the model is not expected to be able to simulate quantitatively all of the observed heat transfer behavior of the supercooler. However, the model should be sufficient to provide some qualitative assessment of the heat transfer characteristics of the supercooler.

The 4-watt heating case will be the basis of the analytical study. Numerical experiments show that a relatively high heat transfer coefficient both at the surface of the AlN and at the bottom of the carbon foam base are needed to correlate the measured temperature rise. The predicted maximum temperature increase for different values of the top heat transfer coefficient  $h_t$  with a bottom heat transfer coefficient  $h_b = 1000$  W/m<sup>2</sup>-K and different top heat transfer coefficient  $h_t$  are compared with the measured data and shown in Figure 11. A top heat transfer of  $h_t = 2000$  W/m<sup>2</sup>-K appears to “fit” the measured maximum temperature increase effectively. When the power is turned off at 30 sec., the model also predicts accurately the rapid temperature reduction observed. The measured temperature distributions obtained by the infrared camera during the heating transient are compared with the COMSOL prediction in Figure 12. The model is

quite effective in capturing the highly localized heating behavior around the heating region.

The relatively high value of the top and bottom heat transfer coefficient (e.g. the typical heat transfer coefficient in air is in the range of 10-100 W/m<sup>2</sup>-K) needed to correlate the experimental data show that the low pressure boiling within the supercooler has a definite role in the cooling process observed. This boiling mechanism, together with the wicking of liquid into the heated region, need to be understood in the future design and improvement of the supercooler.

### **Conclusion and Future Work**

A supercooler is fabricated using carbon foam as the primary heat transfer material for cooling. The carbon foam is soaked with water and the supercooler is operated under evacuated low pressure to ensure that two-phase boiling is occurring to enhance heat transfer. The specific design is directed toward the cooling of a prototypical optoelectronic package in which heat is generated in the order of 1 to 10 W over a region with dimension of 0.5 mm x 5 mm. The corresponding heat fluxes are 40 and 400 W/cm<sup>2</sup>.

Results show that carbon foam and the supercooler are effective in providing high high heat transfer rate at the heating surface. Heat transfer coefficients of 100 kW/(m<sup>2</sup>-K) and 160 kW/(m<sup>2</sup>-K) were observed for the two steady heating cases. The supercooler also shows a remarkable capability of rapid cooling of the heating surface after the heating load is removed. Under periodic heating, the cooling rate for three test frequencies (0.5 Hz, 0.25 Hz and 0.17 Hz) are 17°C/sec, 12°C/sec and 9°C/sec respectively.

A numerical model of the supercooler, excluding the two-phase boiling/condensation effect, is developed using COMSOL. The model is effective in correlating the observed data. However, high heat transfer coefficients are required to obtain agreement with the measured data. An accurate understanding of the two phase flow boiling/condensation process occurring within the carbon foam is clearly needed to to further improve the performance of the supercooler and to adapt the technology to other high heat flux heating scenarios.

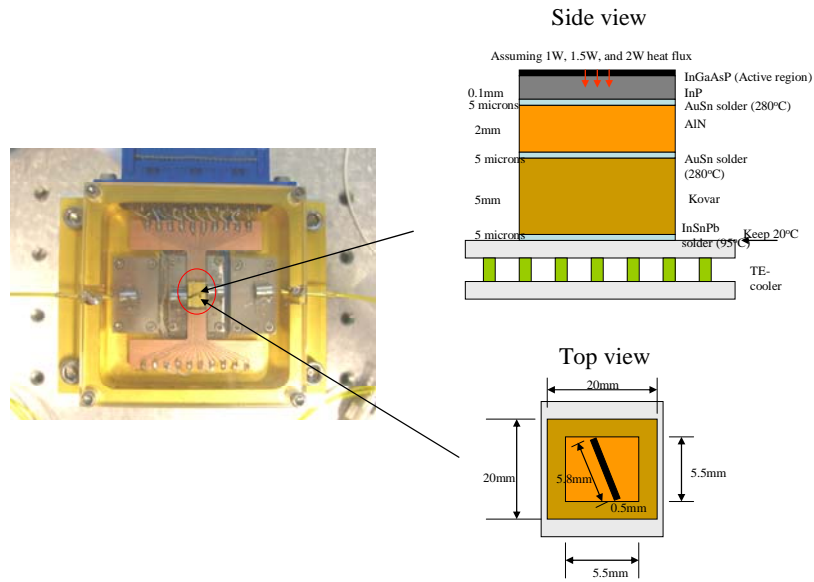


**Figure 1: The prototype electronic package under consideration for cooling by the supercooler.**

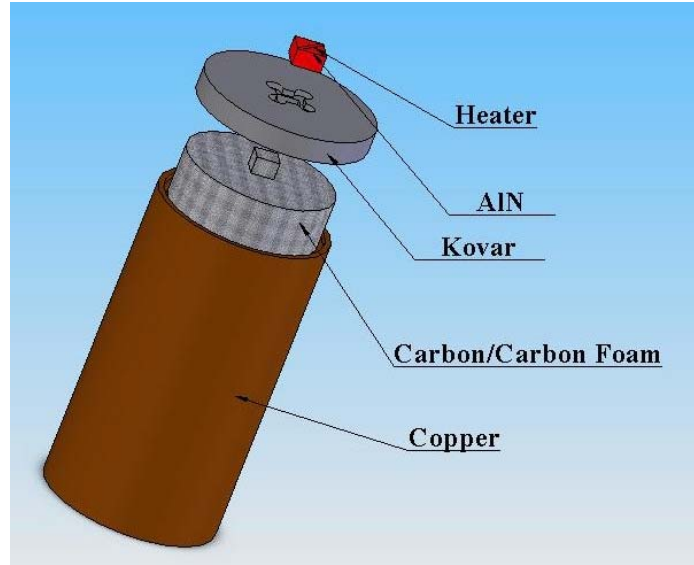
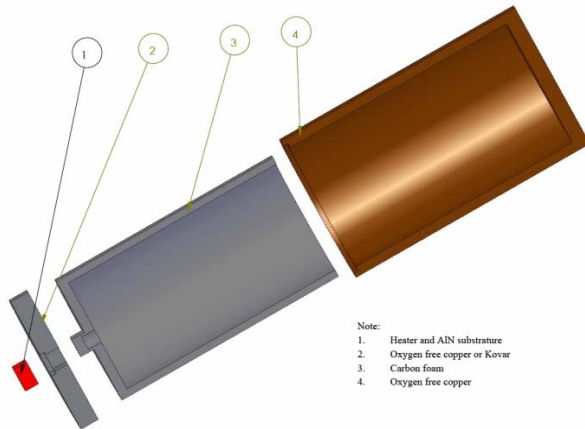


**Figure 2: Schematic of the supercooler.**



- Note:
1. Heater and AlN substrate
  2. Oxygen free copper or Kovar
  3. Carbon foam
  4. Oxygen free copper

**Copper Cover Dimension**

**D = 1.18 in.**

**L = 2.13 in.**

**Thickness of Carbon Foam Shell**

**d = 0.16 in.**

**Figure 3: Interior view of the supercooler and the relevant geometric dimensions.**

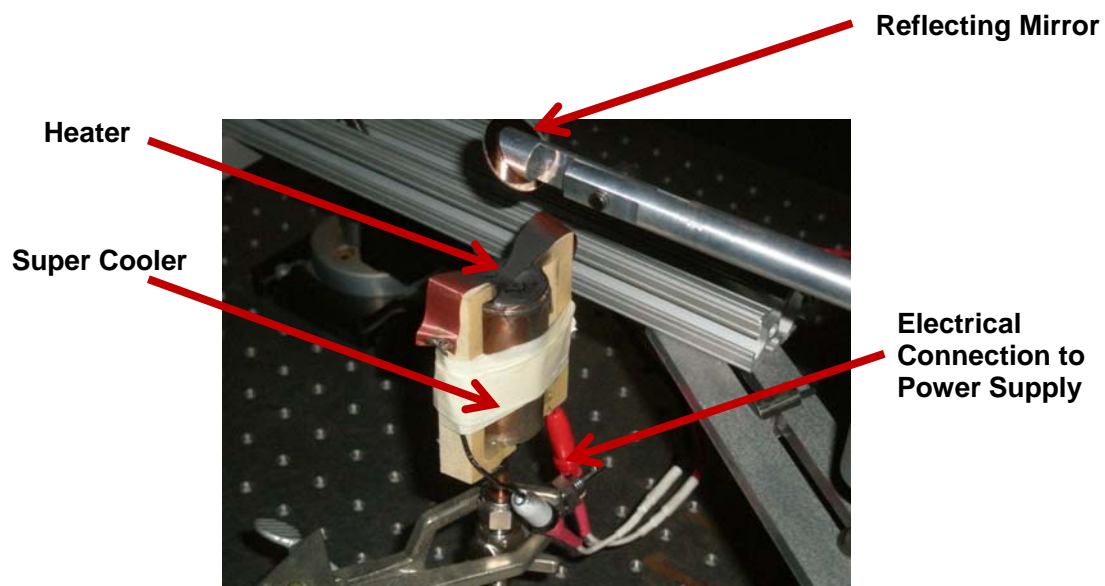


**Figure 4a: Top view of the experimental setup.**

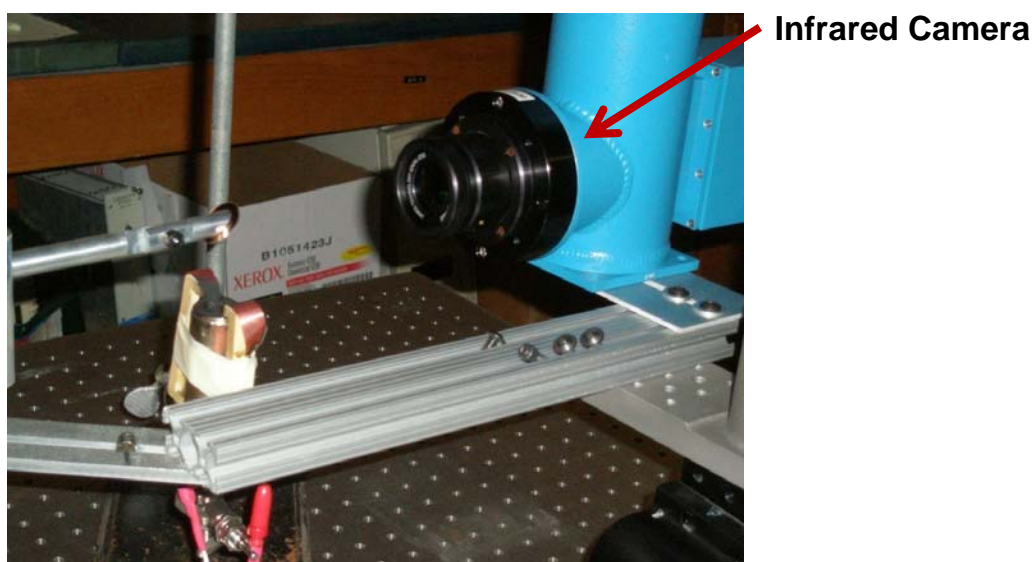


**Figure 4b: Experimental setup, together with the infrared camera used in the temperature measurement.**

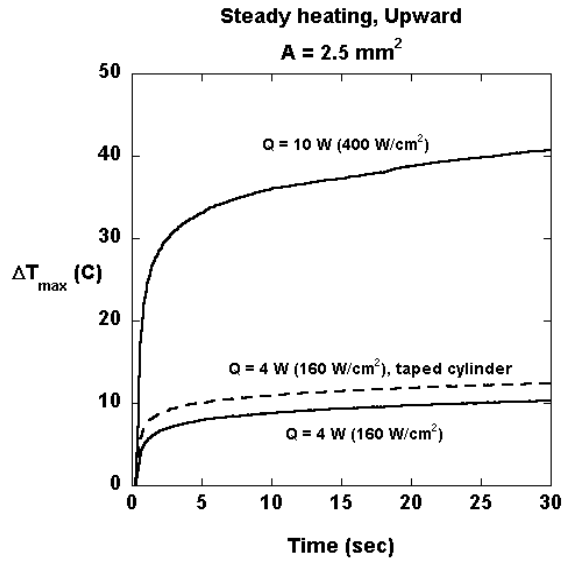


Figure 5a: Effect of heating power for steady heating tests.

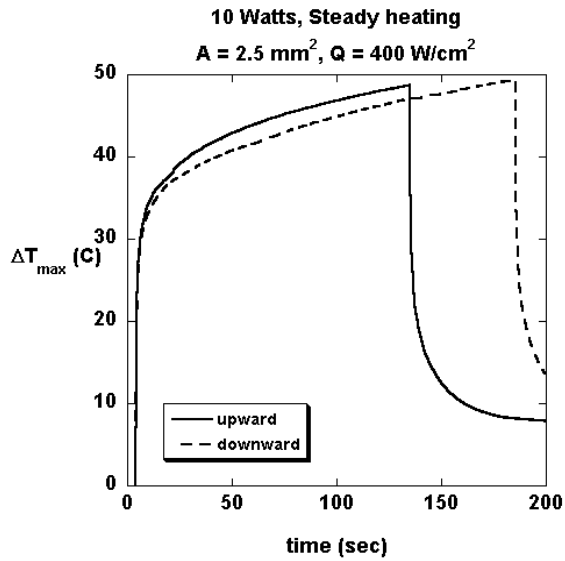
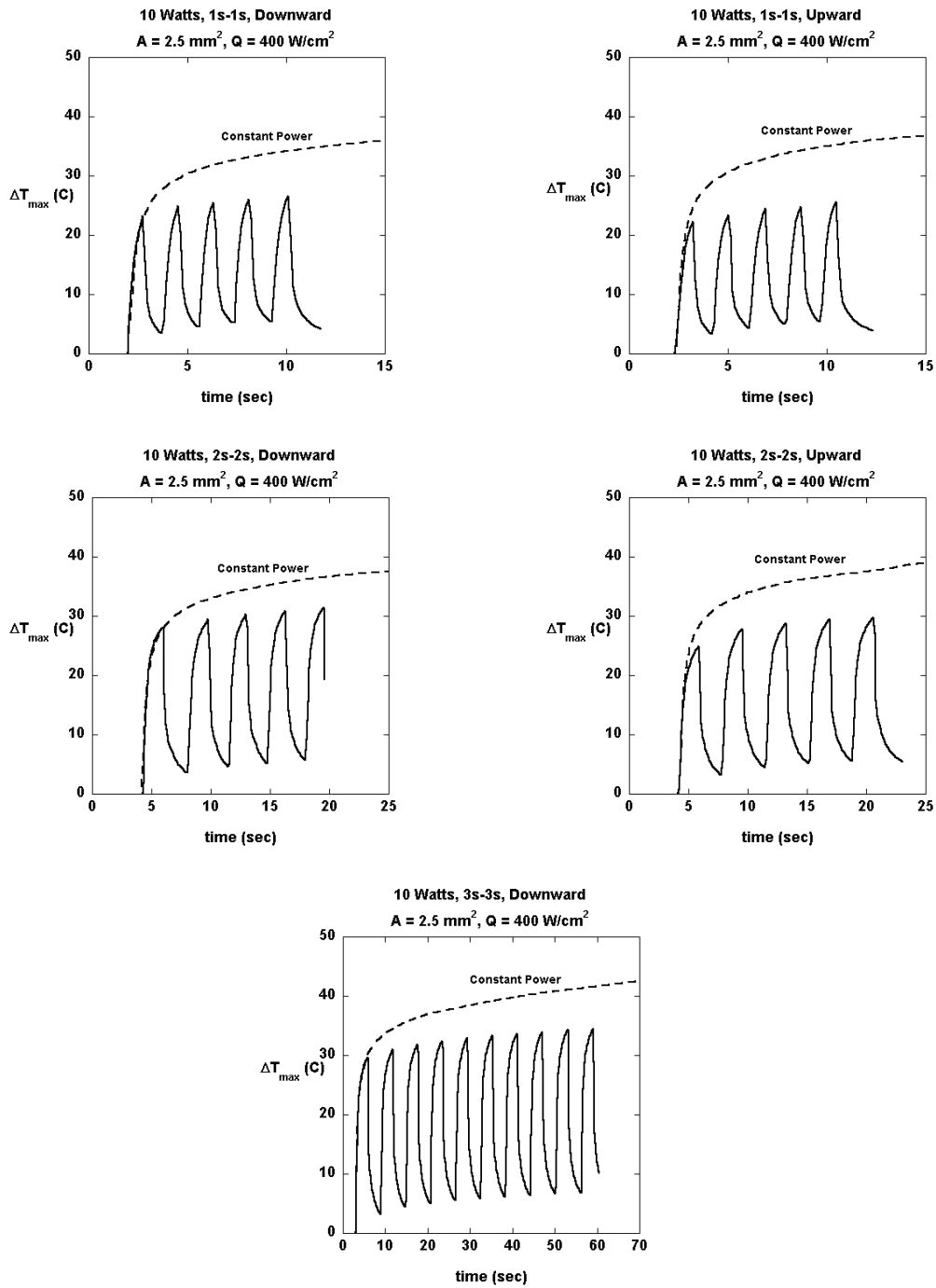
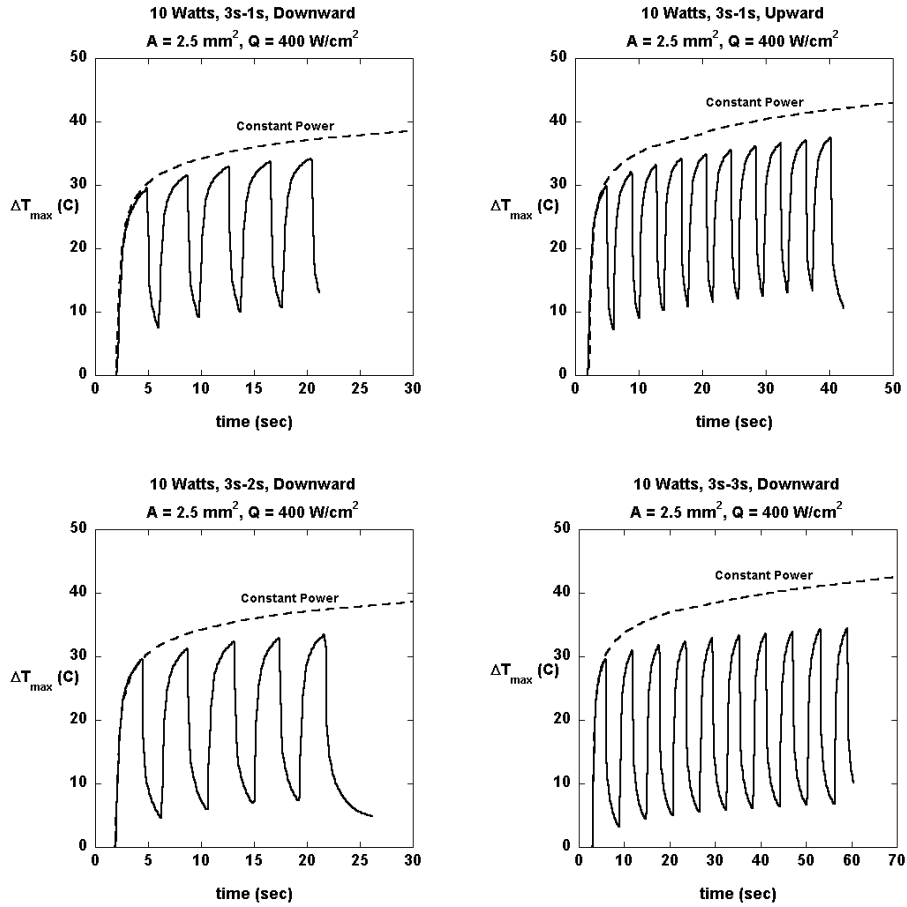


Figure 5b: Effect of heater orientation for the steady heating test with 10 W.



**Figure 6: Measured maximum temperature rise for tests with equal heating and non-heating period with a heating power of 10 W (and a heat flux of  $400 \text{ W/cm}^2$ ). Note that the time identification stands for on-off time period for the test (i.e. 3s-3s stands for the heater is on for 3 sec. and off for 3 sec.).**



**Figure 7: Measured maximum temperature rise for tests with a 3 sec. heating period and different non-heating periods with a heating power of 10 W (and a heat flux of  $400 \text{ W/cm}^2$ ). Note that the time identification stands for on-off time period for the test (i.e. 3s-3s stands for the heater is on for 3 sec. and off for 3 sec.)**

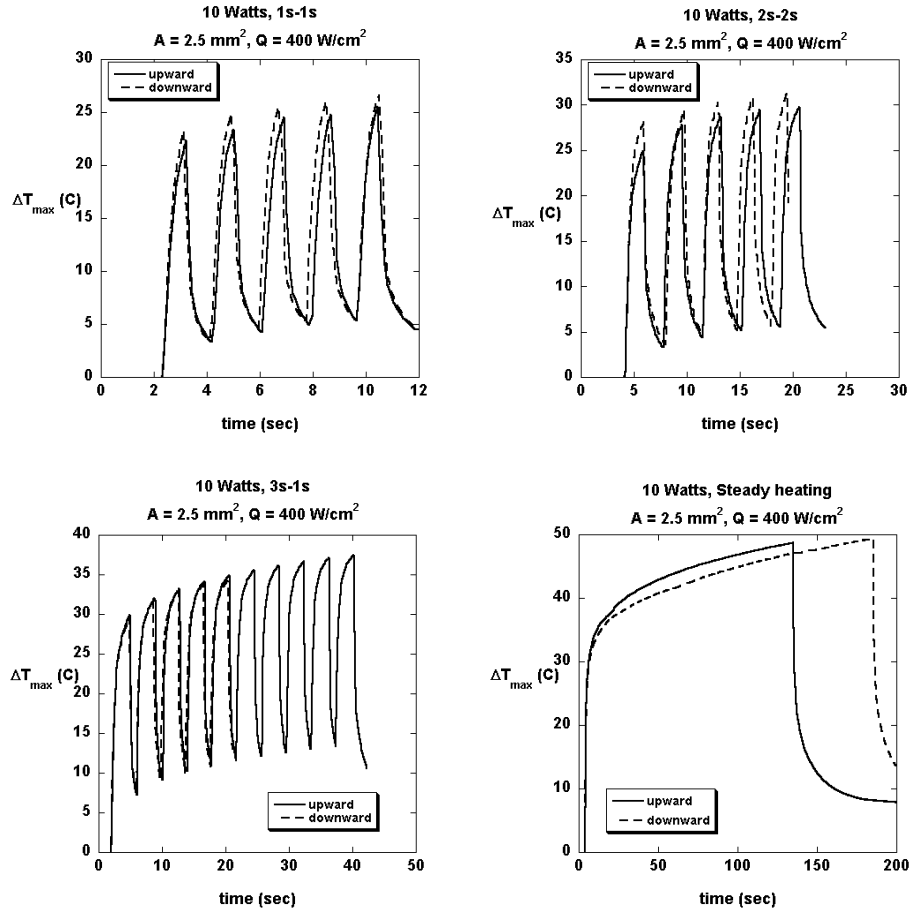


**Figure 8: Effects of heater orientation (downward .vs. upward) for cases with a heating power of 10 W (and a heat flux of  $400 \text{ W/cm}^2$ ). Note that the time identification stands for on-off time period for the test (i.e. 1s-1s stands for the heater is on for 1 sec. and off for 1 sec.)**

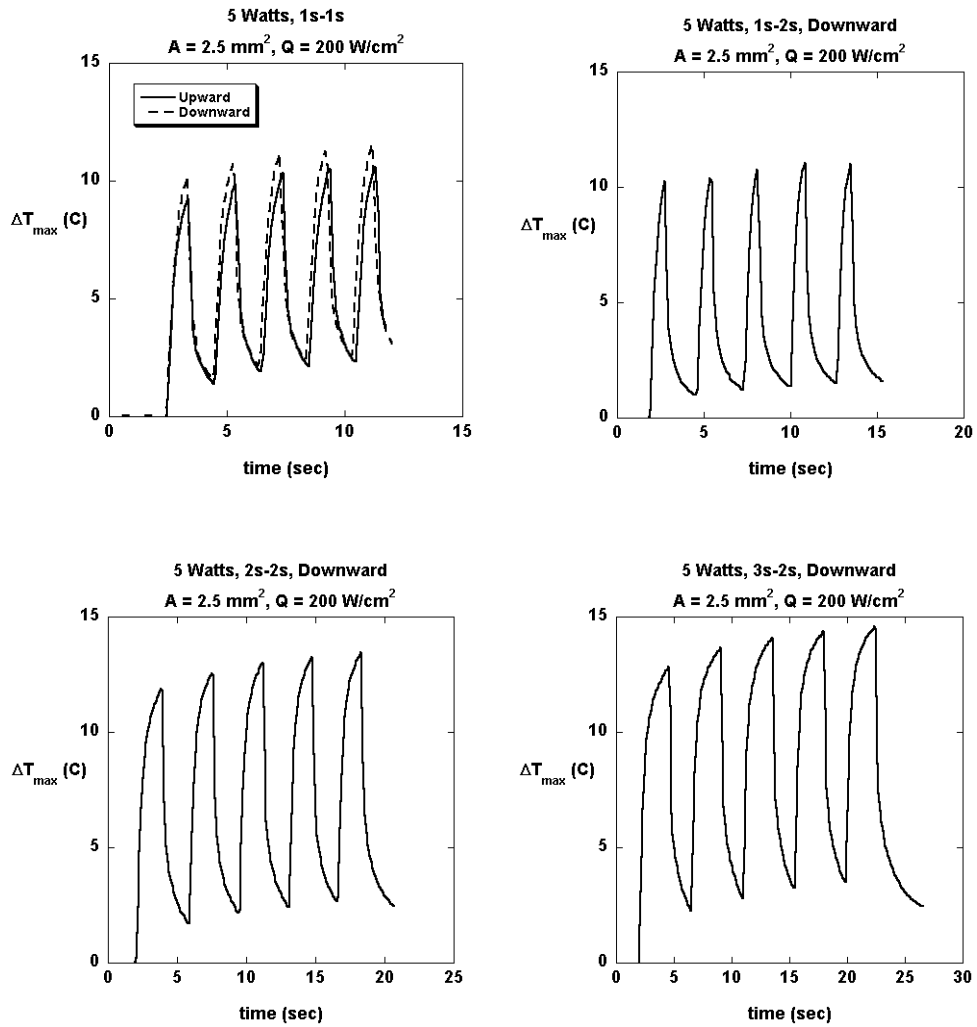


**Figure 9: Measured maximum temperature rise for tests with different heating period and different non-heating periods with a heating power of 5 W (and a heat flux of  $200 \text{ W/cm}^2$ ). Note that the time identification stands for on-off time period for the test (i.e. 1s-1s stands for the heater is on for 1 sec. and off for 1 sec.)**

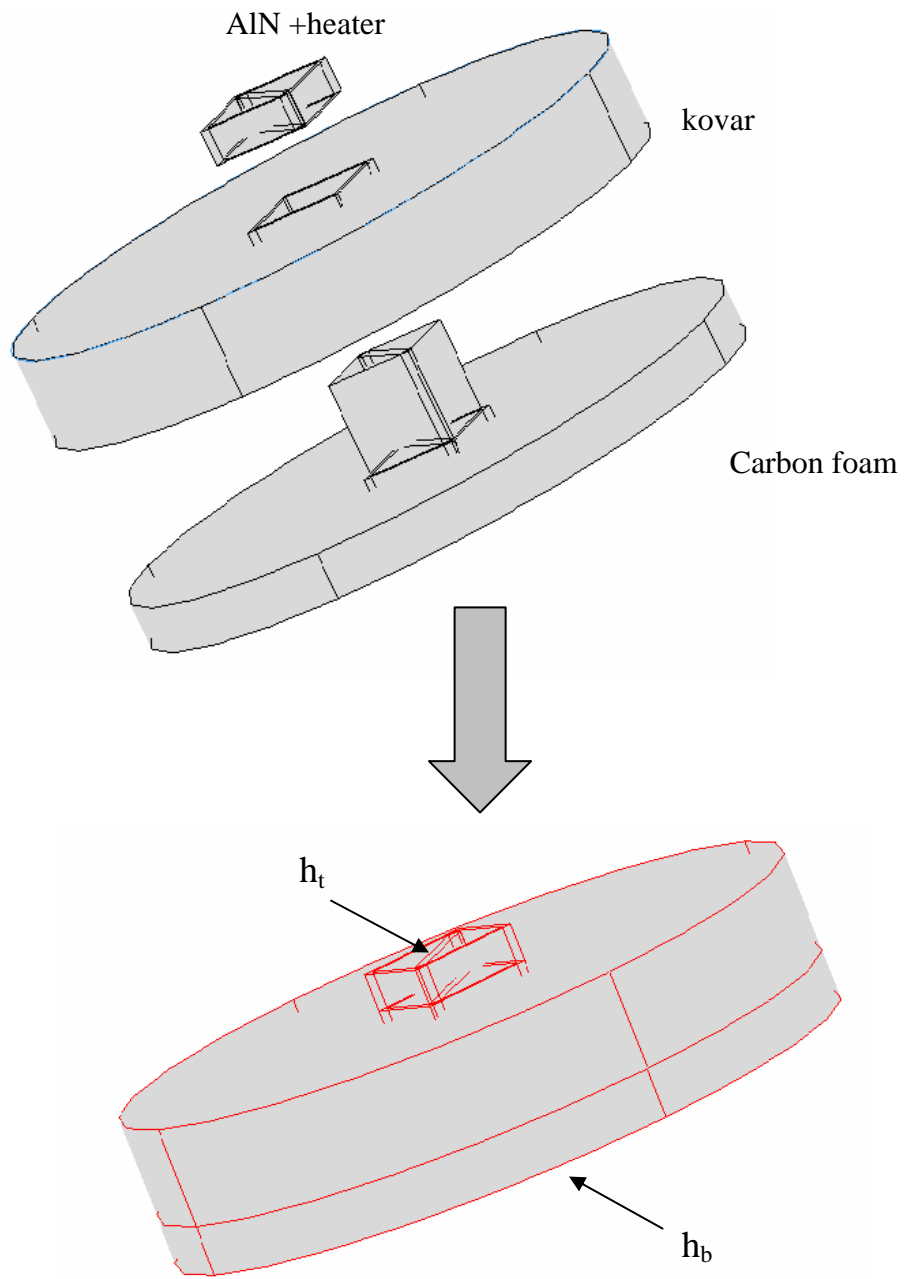


Figure 10: Schematic of the supercooler geometry and the convective heat transfer boundary conditions modeled by COMSOL.

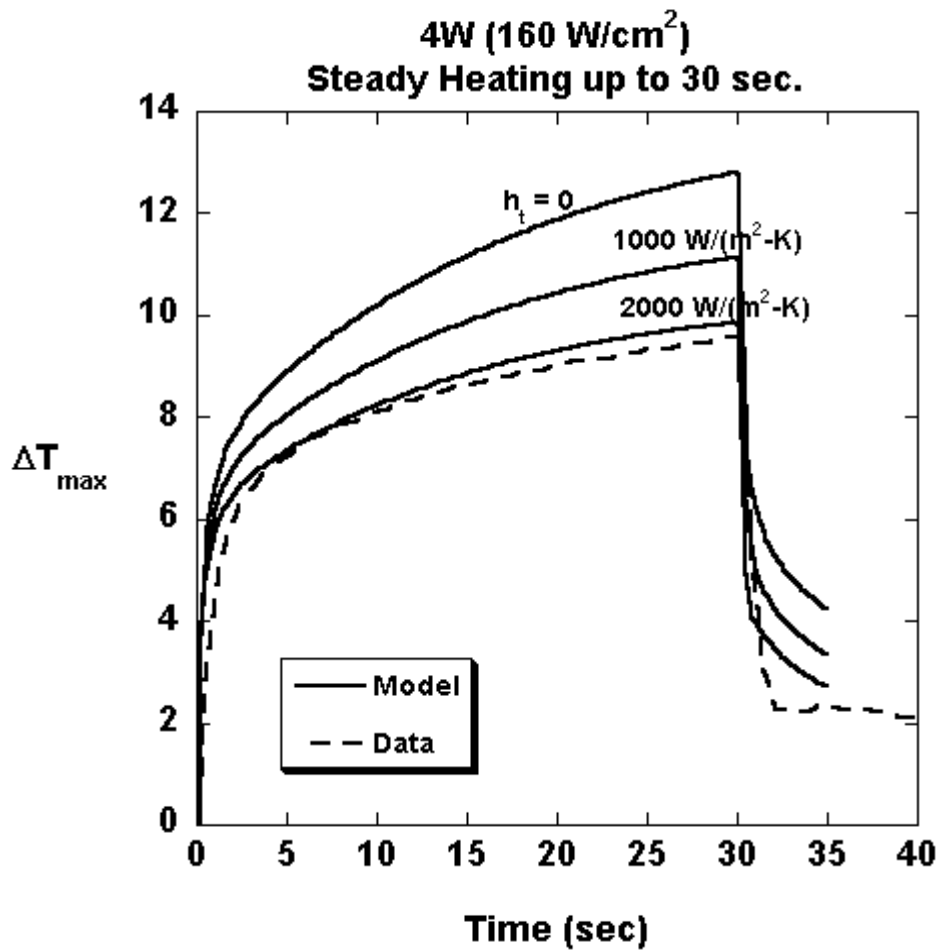
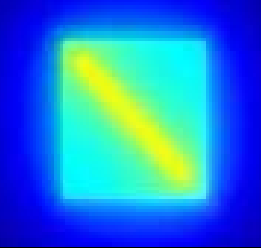
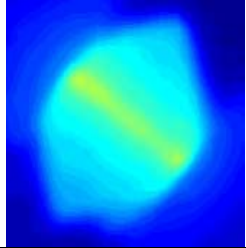
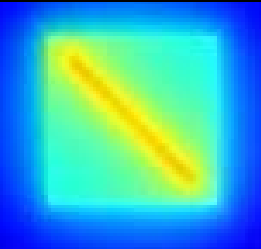
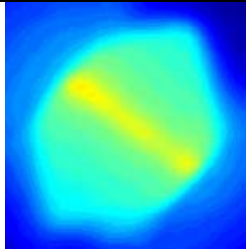
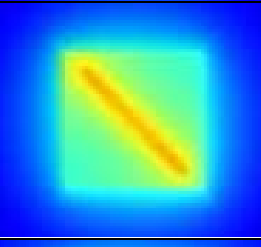
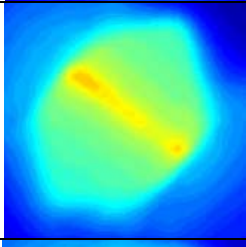
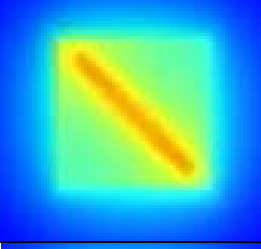
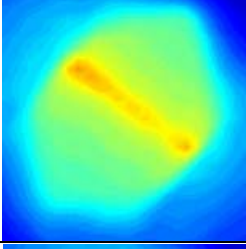
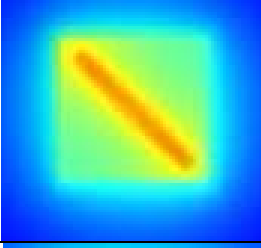
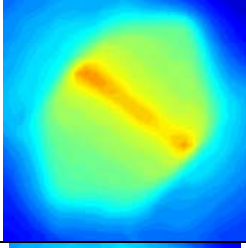
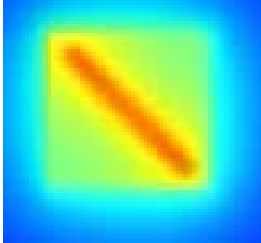
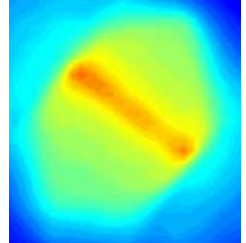
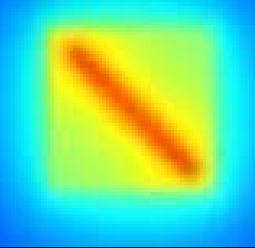
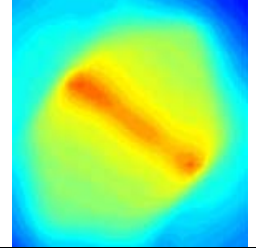
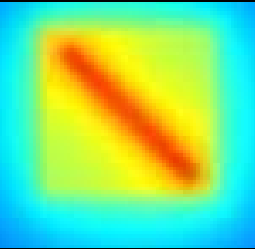
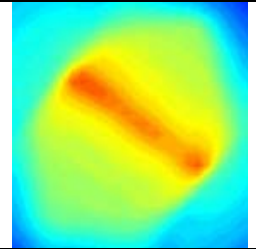
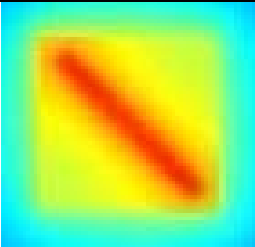
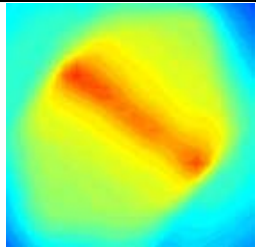
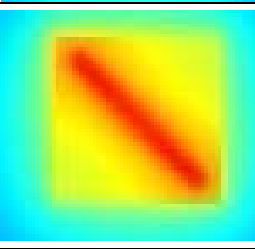
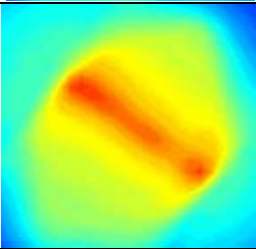
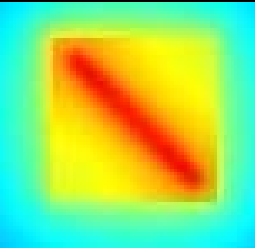
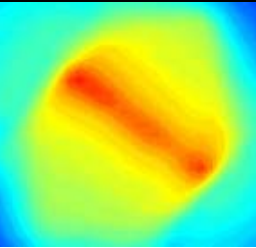
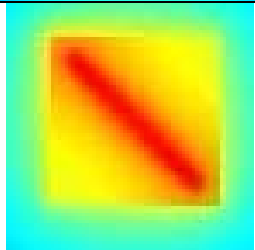
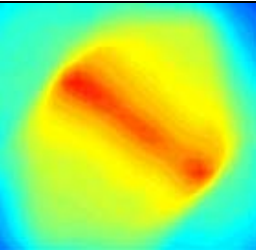
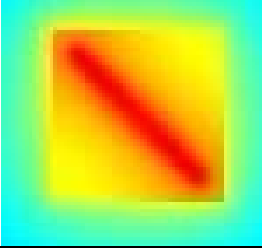
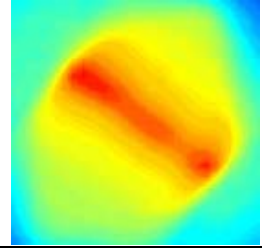
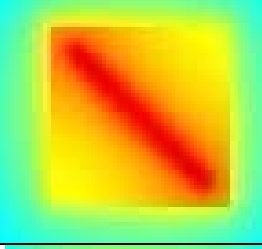
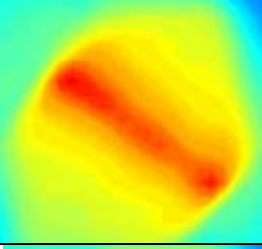
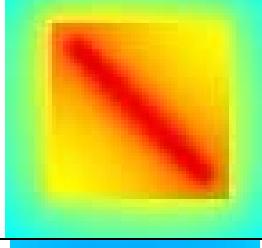
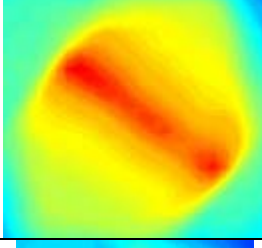
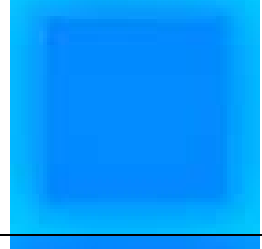
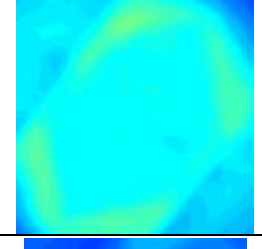
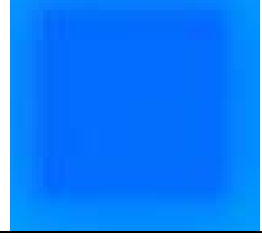
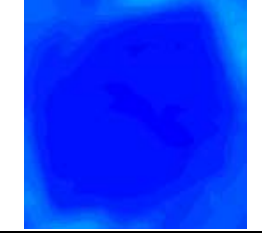


Figure 11: Comparison between the COMSOL prediction of the maximum temperature increase and experiment for different values of the top heat transfer coefficient ( $h_t$ ) with a bottom heat transfer coefficient ( $h_b$ ) of  $1000 \text{ W}/(\text{m}^2\text{-K})$

Time (s)	Model (COMSOL)	Infrared Images
1	 A square heatmap showing a diagonal line of high intensity (yellow) against a blue background.	 A circular infrared image showing a diagonal line of high intensity (yellow) against a blue background.
2	 A square heatmap showing a diagonal line of high intensity (yellow) against a blue background.	 A circular infrared image showing a diagonal line of high intensity (yellow) against a blue background.
3	 A square heatmap showing a diagonal line of high intensity (yellow) against a blue background.	 A circular infrared image showing a diagonal line of high intensity (yellow) against a blue background.
4	 A square heatmap showing a diagonal line of high intensity (yellow) against a blue background.	 A circular infrared image showing a diagonal line of high intensity (yellow) against a blue background.
5	 A square heatmap showing a diagonal line of high intensity (yellow) against a blue background.	 A circular infrared image showing a diagonal line of high intensity (yellow) against a blue background.
7.5	 A square heatmap showing a diagonal line of high intensity (yellow) against a blue background.	 A circular infrared image showing a diagonal line of high intensity (yellow) against a blue background.

Time (s)	Model (COMSOL)	Infrared Images
10	 A square heatmap showing a diagonal band of high intensity (red) from the top-left to the bottom-right, with intensity decreasing towards the corners (blue).	 A circular infrared image showing a diagonal band of high intensity (red) from the top-left to the bottom-right, with intensity decreasing towards the edges (blue).
12.5	 A square heatmap showing a diagonal band of high intensity (red) from the top-left to the bottom-right, with intensity decreasing towards the corners (blue).	 A circular infrared image showing a diagonal band of high intensity (red) from the top-left to the bottom-right, with intensity decreasing towards the edges (blue).
15	 A square heatmap showing a diagonal band of high intensity (red) from the top-left to the bottom-right, with intensity decreasing towards the corners (blue).	 A circular infrared image showing a diagonal band of high intensity (red) from the top-left to the bottom-right, with intensity decreasing towards the edges (blue).
17.5	 A square heatmap showing a diagonal band of high intensity (red) from the top-left to the bottom-right, with intensity decreasing towards the corners (blue).	 A circular infrared image showing a diagonal band of high intensity (red) from the top-left to the bottom-right, with intensity decreasing towards the edges (blue).
20	 A square heatmap showing a diagonal band of high intensity (red) from the top-left to the bottom-right, with intensity decreasing towards the corners (blue).	 A circular infrared image showing a diagonal band of high intensity (red) from the top-left to the bottom-right, with intensity decreasing towards the edges (blue).
22.5	 A square heatmap showing a diagonal band of high intensity (red) from the top-left to the bottom-right, with intensity decreasing towards the corners (blue).	 A circular infrared image showing a diagonal band of high intensity (red) from the top-left to the bottom-right, with intensity decreasing towards the edges (blue).

Time (s)	Model (COMSOL)	Infrared Images
25		
27.5		
30		
31		
32		

**Figure 12: Comparison between two-dimensional temperature distribution around the heater at different time as predicted by COMSOL (left) and measurement by the infrared camera (right)**